Atomic-Resolution in Situ Transmission Electron Microscopy of a Promoter of a Heterogeneous Catalyst

Thomas W. Hansen,[1] Jakob B. Wagner,[1,2] Poul L. Hansen,[1]
Søren Dahl,[1] Haldor Topsøe,[1] Claus J. H. Jacobsen[1]*

Insight into the location, state, and function of a promoter in heterogeneous catalysis was obtained through atomic-resolution in situ transmission electron microscopy. In the most active ruthenium catalyst for ammonia synthesis known so far, the barium promoter is shown to be located in two different phases in the catalyst. The increased activity is suggested to be related to a two-dimensional barium-oxygen overlayer on the ruthenium crystals. The possibility for conducting such studies for other reactions could add substantially to our current understanding of heterogeneous catalysis. Heterogeneous catalysis plays an increasingly important role in environmental protection processes, in fuel upgrading, and in providing the majority of the chemical building blocks required by contemporary society. Most heterogeneous catalysts of industrial importance are multicomponent materials that are designed by trial-and-error experimentation. Application of even the most sophisticated physical-chemical characterization techniques is usually not sufficient to obtain a complete understanding of the structure of the active site, the reaction mechanism and kinetics, the structural dynamics, and the specific roles of all catalyst components.

Various in situ characterization methods that allow studies of heterogeneous catalysts under realistic reaction conditions have substantially improved our possibilities for obtaining relevant structural information (*1–3*). Also, the use of surface science techniques (*4–6*) and theoretical modeling (*7–9*) has recently added substantially to our understanding of heterogeneous catalysis. In many industrial catalyst systems, the presence of so-called catalyst promoters is essential to achieve the required activity or selectivity. Usually, a promoter is defined as a substance that causes a more than proportional increase in activity or selectivity when added to the catalyst (*10*). In many cases, the promoter alone is completely inactive in the catalytic process, where it is used to boost productivity. It is common practice to distinguish between structural promoters that cause an increase in the number of active sites and electronic promoters that produce active sites with a higher intrinsic activity, i.e., higher turnover frequencies. In early studies, Mittasch performed systematic studies of the influence of various catalyst promoters with ammonia synthesis catalysts (*11*). Previously, the influence of such "impurities" had only been observed more or less inadvertently. Although the effect of the promoter on the catalytic activity and reaction kinetics is easily measured, structural information is rarely available. Very often, electronic promoters are present in relatively small amounts and are not found as crystalline structures, which complicates the structural characterization. More importantly, the promoter is often distributed between various phases of the catalyst, making the establishment of structure-activity relations very difficult.

We now show how atomic-resolution in situ transmission electron microscopy (TEM) can be used to obtain insight into the structure of barium-promoted ammonia synthesis catalysts. We also show how it is necessary to combine atomic-resolution in situ TEM with theoretical modeling and other characterization techniques to understand the dramatic influence of the promoter on the catalytic activity and to elucidate the location and state of the barium promoter. The studies are conducted with a recently developed barium-promoted ruthenium catalyst on a support of boron nitride (Ba-Ru/BN) that was shown to exhibit unprecedented activity and stability in catalytic ammonia synthesis (*12*).

Catalytic activity measurements with both Ru/BN and Ba-Ru/BN were performed as previously described (*13*). After testing, the catalysts were passivated and transferred to the TEM facility. The conventional TEM images are obtained on a Philips CM-200 FEG microscope with an UltraTwin lens giving a resolution limit of about 0.12 nm. A Philips CM-300 microscope equipped with a SuperTwin lens with a resolution limit of 0.14 nm was used for the in situ studies (*14*).

For in situ studies, the catalyst was treated in the in situ cell with a 3:1 H_2/N_2 mixture at 550°C and 5.2 mbar for 30 min. These conditions were sufficient for complete reduction of the passivated catalyst samples. For each catalyst studied, more than 100 images were obtained and no other structures than those described were observed. Thus, the images shown were selected only to give the best representation of the surface structures. The catalytic activity of the 4.5 weight (wt) % Ru/BN catalysts is measured in a plug flow reactor at 400°C and 50 bar in a 3:1 mixture of H_2 and N_2. At an NH_3 outlet concentration of 1.2%, an integral reaction rate of 2.2 μmol g^{-1} s^{-1} is obtained. This rate is comparable to the activity previously reported for 5.4 wt % Ru/graphite at the same

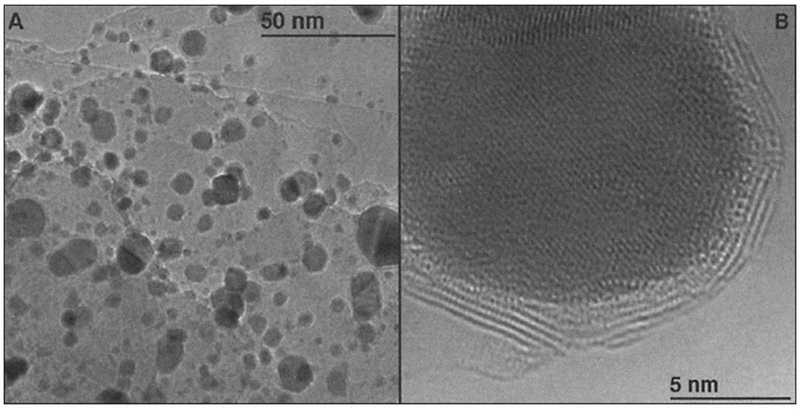

Fig. 1. Representative conventional TEM images of Ba-promoted Ru catalyst supported on BN. (**A**) Low-magnification image showing Ru crystals on the hexagonal BN support. A thin film of BN covers most Ru crystals. (**B**) High-magnification image showing the three to four layers of BN covering a Ru crystal. The distance between the BN layers is 0.34 nm corresponding to the (002) planes. The lattice spacings seen in the Ru particle are 0.23 nm in two directions 60° from each other, indicating that the zone axis is [001].

---

[1]Haldor Topsøe A/S, Nymøllevej 55, DK-2800 Lyngby, Denmark. [2]Niels Bohr Institute for Astronomy, Physics, and Geophysics, University of Copenhagen, Universitetsparken 5, DK-2100 Copenhagen Ø, Denmark.

*To whom correspondence should be addressed. E-mail: chj@topsoe.dk

conditions (*13*). Upon promotion with 5.5 wt % barium, an integral reaction rate of 32.8 μmol g^{-1} s^{-1} was achieved at 400°C and 50 bar at an NH_3 outlet concentration of 8.4%. Taking the NH_3 inhibition into account, the activity increase is more than two orders of magnitude. Figure 1 shows images of the Ba-Ru/BN catalyst obtained with conventional TEM, which show how all of the Ru crystals are completely covered by the support material. Lattice fringes are resolved in both the Ru particles and BN support material. The hexagonal BN used as a support for the present catalysts has a structure closely related to that of graphite. On the basis of H_2 adsorption experiments, it has previously been suggested for graphite-supported Ru catalysts for NH_3 synthesis that the graphite partly covers the Ru crystals (*15*). Although energy-dispersive spectroscopy can verify the presence of Ba in the catalyst, it is not possible to identify any Ba-rich phases in the TEM images. However, it does not appear that Ba is primarily present on the Ru crystals.

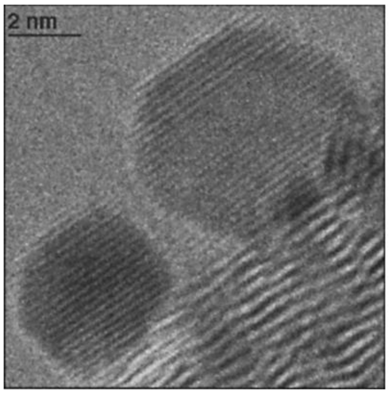

Fig. 2. Representative in situ TEM image of the unpromoted Ru catalyst recorded at a temperature of 331°C and a pressure of 3.0 mbar in a gas composition H_2/N_2 of 3:1. No surface features are seen on any of the Ru crystals. The lattice spacing is 0.21 nm corresponding to the (101) planes. The Ru crystals show well-developed facets.

From the conventional TEM studies, it is not possible to obtain insight into the location and mode of operation of the Ba promoter, and it is even difficult to see how the catalyst can be active when the Ru crystals are completely covered by several layers of BN. Therefore, we decided to study the same catalyst in the in situ TEM facility. Initially, we studied the unpromoted Ru/BN catalyst. Figure 2 shows Ru crystals supported on BN at 331°C and 3.0 mbar of 3:1 H_2/N_2. Under these conditions, the BN is not covering the Ru crystals. Still, the crystal lattice of Ru is well-resolved just as the layered structure of BN could be easily observed. Most crystals exhibit a hexagonal morphology that was observed previously in conventional TEM studies of supported Ru catalysts for NH_3 synthesis (*13*). During activation of the catalyst in the microscope, small Ru crystals with a size below 1 nm are observed to diffuse over the flat part (the terraces) of the BN surface. The coalescence (sintering) of such small crystals into larger crystals of about 2.0 nm can be followed directly. It has been suggested that such sintering is necessary to form crystals of an optimum size around 2.0 nm that exhibit the highest number of active B_5-type sites primarily located at crystal edges and corners (*13*). On the basis of microkinetic modeling of a $Ru/MgAl_2O_4$ catalyst with the same activity as the Ru/BN catalyst, it has previously been estimated that about 9% of the Ru surface sites are active in NH_3 synthesis (*16*).

Upon introduction of the Ba promoter, an increase of about two to three orders of magnitude in catalytic activity was observed. As can be seen from the in situ TEM images in Fig. 3, the morphology of the Ru crystals was not altered by the presence of Ba, which suggests that the number of active sites was not substantially altered and that Ba is an electronic promoter (although it has recently been suggested that Ba might be a structural promoter) (*17*). In the in situ TEM images, two distinctly new structures can be seen on the exterior of the Ru crystals in the Ba-promoted catalyst. One such structure is an amorphous Ba-containing phase that covers a substantial fraction of some faces of the Ru crystals. Another is a well-dispersed structure that can only be observed in the atomic-resolution in situ TEM. It appears that the Ba atoms are quite mobile under NH_3 synthesis conditions. In situ electron energy-loss spectroscopy (EELS) at the O K edge and the Ba $M_{4,5}$ edge demonstrates that the Ba is present in an oxide structure. Usually, electronic promoters in NH_3 synthesis are thought to reside as oxygen-containing adlayers on the metal crystals, although this idea is still controversial (*18*). It is not clear how the electronic promoters exert their dramatic influence on the NH_3 synthesis activity; several different locations have been suggested for promoters on Ru catalysts (*19*). For the Ba-Ru/BN catalyst, two different structures containing promoter atoms were observed, and from the TEM studies alone, it is not possible to conclude which is related to the increased activity. However, recent density functional theory studies have shown that the activity of both unpromoted (*9*, *20*, *21*) and promoted (*22*) NH_3 synthesis catalysts is related to the presence of B_5-type sites. For the unpromoted catalyst, this finding has been experimentally supported by single-crystal studies (*23*).

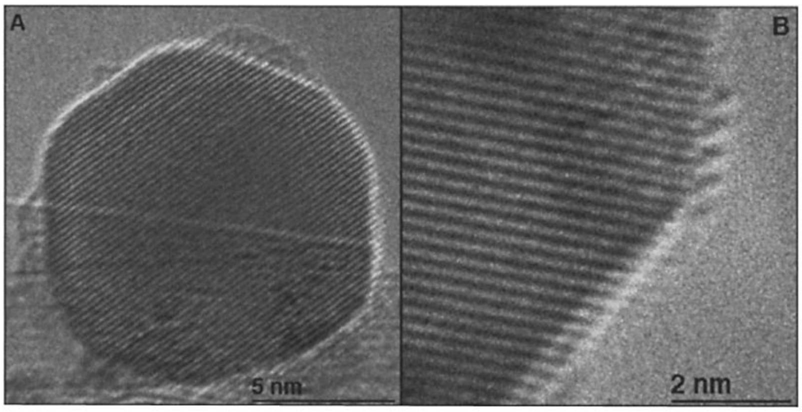

Fig. 3. In situ images of the Ba-promoted Ru catalyst recorded at 552°C and 5.2 mbar in a gas composition H_2/N_2 of 3:1. (**A**) Patches of a Ba-containing phase are found on several of the Ru crystal surfaces. The lattice spacing in the Ru particle is 0.21 nm corresponding to the (101) planes. (**B**) High-magnification image of the edge of a Ru crystal. The lattice spacing is 0.23 nm, i.e., the (100) planes of Ru. On the edge of the Ru crystal, a small monolayer patch of a barium oxide phase is observed. The distance between the dark spots representing the Ba atoms is 0.48 nm.

We suggest that the Ba atoms distributed as single atoms close to the crystal edges (B_5 sites) and bound to oxygen are responsible for the electronic promotion of the catalyst. Only very few of such active sites are present in the catalyst, but the optimal promotion of Ru catalysts typically occurs at the relatively large promoter/Ru ratios of 0.3 to 2.0 (atom/atom) (*15*, *24*, *25*). Therefore, it appears that the Ba-containing structures observed on many crystals are reservoirs needed to maintain a constant coverage of mobile Ba atoms in the vicinity of all B_5-type sites in the catalyst. Otherwise, it should be possible to achieve the promotion with a substantially smaller amount of the electronic promoter.

We conclude that conventional TEM studies are not optimally suited for detailed studies of heterogeneous catalysts. Particularly for studies of electronic promoters, atomic-resolution in situ TEM may be the only technique that allows direct imaging of the promoter structures during catalyst operation. It appears that similar studies could be used to obtain a more detailed understanding of the role of promoters in other catalyst systems, such as alkali-promoted catalysts for steam reforming, Fischer-Tropsch synthesis, and olefin epoxidation.

References and Notes

1. G. Ertl, H. Knözinger, J. Weitkamp, Eds., *Handbook of Heterogeneous Catalysis* (VCH, Weinheim, Germany, 1997).

2. J. W. Niemantsverdriet, *Spectroscopy in Catalysis* (Wiley-VCH, Weinheim, Germany, 1993).
3. H. Topsøe, *Stud. Surf. Sci. Catal.* **130**, 1 (2000).
4. G. Ertl, H.-J. Freund, *Phys. Today* **52**, 32 (January 1999).
5. G. A. Somorjai, *Introduction to Surface Chemistry and Catalysis* (Wiley, New York, 1994).
6. J. V. Lauritsen *et al.*, *J. Catal.* **197**, 1 (2001).
7. R. A. van Santen, M. Neurock, *Catal. Rev.* **37**, 557 (1995).
8. P. Raybard, J. Hafner, G. Kresse, S. Kasztelan, H. Toulhoat, *J. Catal.* **190**, 128 (2000).
9. A. Logadottir *et al.*, *J. Catal.* **197**, 229 (2001).
10. Z. Paal, G. A. Somorjai, in *Handbook of Heterogeneous Catalysis*, G. Ertl, H. Knözinger, J. Weitkamp, Eds. (VCH, Weinheim, Germany, 1997), vol. 3, pp. 1084–1104.
11. A. Mittasch, *Adv. Catal.* **2**, 81 (1950).
12. C. J. H. Jacobsen, *J. Catal.* **200**, 1 (2001).
13. C. J. H. Jacobsen *et al.*, *J. Mol. Catal. A.* **163**, 19 (2000).
14. This microscope has a Gatan image filter for EELS studies and for recording energy-filtered images. The in situ system consists of an environmental cell pumped differentially by a molecular drag pump in the first pumping stage and a turbomolecular pump in the second stage. The design of the environmental cell is adopted from Boyes and Gai at DuPont (*26*) and constructed by Philips in collaboration with Haldor Topsøe A/S. The in situ cell allows heating and introduction of a controlled, gaseous environment over the sample. A resolution better than 0.16 nm can be achieved at pressures of about 20 mbar and temperatures of about 900°C (dependent on gas pressure and composition).
15. Z. Kowalczyk *et al.*, *Appl. Catal. A* **184**, 95 (1999).
16. S. Dahl, J. Sehested, C. J. H. Jacobsen, E. Törnqvist, I. Chorkendorff, *J. Catal.* **192**, 391 (2000).
17. W. Rarog, Z. Kowalczyk, J. Sentek, D. Skladanowski, J. Zielinski, *Catal. Lett.* **68**, 163 (2000).
18. G. A. Somorjai, N. Materer, *Top. Catal.* **1**, 215 (1994).
19. S. Tennison, in *Catalytic Ammonia Synthesis*, J. R. Jennings, Ed. (Plenum, New York, 1991), pp. 303–364.
20. J. J. Mortensen, L. B. Hansen, B. Hammer, J. K. Nørskov, *J. Catal.* **182**, 479 (1999).
21. S. Dahl *et al.*, *Phys. Rev. Lett.* **83**, 1814 (1999).
22. S. Dahl, A. Logadottir, C. J. H. Jacobsen, J. K. Nørskov, *Appl. Catal.*, in press.
23. S. Dahl, E. Törnqvist, I. Chorkendorff, *J. Catal.* **192**, 381 (2000).
24. L. Forni, D. Molinari, I. Rossetti, N. Pernicone, *Appl. Catal. A* **185**, 269 (1999).
25. H. Bielawa, O. Hinrichsen, A. Birkner, M. Muhler, *Angew. Chem.* **113**, 1093 (2001).
26. E. D. Boyes, P. L. Gai, *Ultramicroscopy* **67**, 219 (1997).
27. We gratefully acknowledge the participation of the CTCI Foundation, Taiwan, in the establishment of the TEM facilities. J.B.W. thanks the Danish Research Academy for supporting a scholarship at the Interdisciplinary Research Center for Catalysis (ICAT), Technical University of Denmark.

16 July 2001; accepted 12 October 2001

Seismic Evidence of an Extended Magmatic Sill Under Mt. Vesuvius

Emmanuel Auger,[1] Paolo Gasparini,[1] Jean Virieux,[2] Aldo Zollo[1]

Mt. Vesuvius is a small volcano associated with an elevated risk. Seismic data were used to better define its magmatic system. We found evidence of an extended (at least 400 square kilometers) low-velocity layer at about 8-kilometer depth. The inferred *S*-wave (~0.6 to 1.0 kilometer per second) and *P*-wave velocities (~2.0 kilometer per second) as well as other evidence indicate an extended sill with magma interspersed in a solid matrix.

Mt. Vesuvius is a strato volcano near a densely populated area. It is located in a tectonic graben formed in the Plio-Pleistocene, and it is only a few km southeast of Fields, the active volcano on which the city of Napoli has been built (Fig. 1). It experienced at least three violent explosive eruptions in historical times (79, 472, and 1631 A.D.). More frequent, less explosive eruptions have occurred from 1631 to 1944 (*1*). Mt. Vesuvius is presently in a quiescent state, characterized by low-temperature fumaroles (less than 100°C) and moderate seismic activity (about 100 earthquakes per year with magnitudes between 0.5 and 3.6), and it is difficult to predict when it may erupt explosively again. The definition of its structure and of the location and volume of the magma reservoir can be used to help prediction of the scenario of the next eruption and to interpret the pattern of the expected precursory seismic activity and ground deformation. The present volcanic edifice was built in a time span of about 40,000 years, and the total amount of erupted magma can be estimated to be about 50 km³. This would be the minimum volume of the magma reservoir if it was a closed system. However, Sr, Nd, Pb, and U-Th-Ra data indicate that the magma system underwent a complex, multistage evolution, which is not compatible with a closed magma reservoir (*2*–*7*).

Indications of the lithostatic pressure (and hence the depth) under which the Mt. Vesuvius magmas began to crystallize can be obtained from fluid inclusions in phenocrysts and from mineral equilibria in skarn rocks, which are believed to be formed by high-temperature metamorphism of the carbonate wall rocks. Application of these methods to the products of the last eruptions of Mt. Vesuvius (1906 and 1944) suggests the presence of a magma reservoir at less than 3-km depth refilled during the eruptions with magma coming from a deeper (11 to 22 km) reservoir (*8*, *9*). Fluid inclusions in older Mt. Vesuvius explosive and effusive products indicate crystallization depths between 4 and 10 km (*10*).

A seismic tomography study carried out in

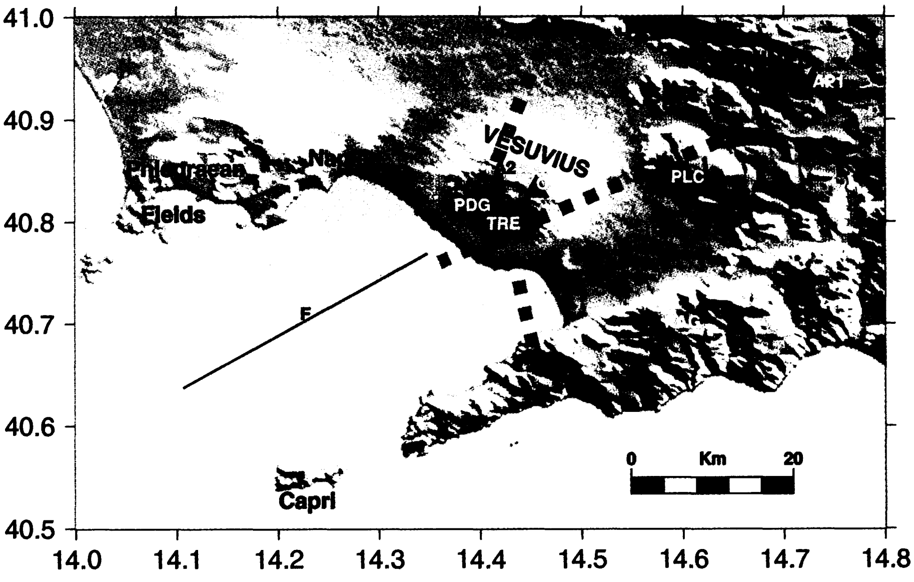

Fig. 1. Sketch map of Mt. Vesuvius area. The black line (F profile of the MAREVES experiment) indicates the profile where the LALA phase is best observed. Blue triangles and three-letter symbols indicate the location of on-land stations of the MAREVES experiment. The gray boxes indicate the points of the mid-crustal interface where the observed LALA phases are generated. They do not correspond to the common midpoint because of *P* to *S* conversion.

---

[1] Dipartimento di Scienze Fisiche, Università di Napoli Federico II, Complesso di M. S. Angelo, Via Cinthia, 80124 Napoli, Italy. [2] Géosciences Azur, 250 Avenue A. Einstein, 06560 Valbonne, France.